GeoAmericas2020
4th PAN AMERICAN CONFERENCE ON GEOSYNTHETICS
26-29 APRIL 2020 • RIO DE JANEIRO • BRAZIL

Lateral Displacements in Geosynthetic-Reinforced Soil Structures with Segmental-Block Facing Systems

A.M. Morsy, Parsons Corporation, Syracuse, New York, USA; Cairo University, Giza, Egypt.
J.G. Zornberg, The University of Texas at Austin, Austin, Texas, USA.
B.R. Christopher, Christopher Consultants, St. Augustine, Florida, USA.
D. Leshchinsky, ADAMA Engineering, Clackamas, Oregon, USA; University of Delaware, Newark, Delaware, USA.

ABSTRACT
Current design criteria for geosynthetic-reinforced soil walls are generally based on factored load and resistance norms, for both internal and external stability analyses, which refer to the ultimate limit state. The serviceability limit state is generally overlooked in the design of geosynthetic-reinforced soil walls, especially for those with facing systems that are comparatively flexible, including segmental retaining wall systems. Serviceability limit design is deemed crucial for critical structures or structures where the consequences of significant deflections are important. This paper presents a lateral displacement model for geosynthetic-reinforced soil structures. The model takes a model commonly used in current practice as initial basis; the original model has been used by practitioners merely to obtain preliminary estimates of lateral displacements in reinforced soil structures during construction. Lateral displacement data from several carefully selected free standing walls with surcharge were collected during construction as a function of the corresponding loads (from the successive layers and from surcharge or bridge loads). The collected data were used to empirically develop the lateral displacement model. The refined model presented in this paper accounts for the geometry and global stiffness of reinforced soil walls constructed both with and without surcharge loads.

1. INTRODUCTION

Over the centuries, civil engineers have focused on expanding the infrastructure assets as well as introducing new technologies into our infrastructure. Recently, our community have faced challenges to maintain our assets as well as to catch up with the ever-growing infrastructural demand. This is because our infrastructure assets degrade and require rehabilitation and replacement in the meantime that the size of assets need to increase to satisfy the needs of our communities. These challenges implore for development of innovative and sustainable solutions that consider not only cost, safety, and serviceability, but also resilience, environment, and public acceptance. That is, the number of the main variables in the decision-making process that require reconciliation needs to increase to arrive to sustainable solutions that capitalizes the use of our current and future infrastructure assets. A major component with in the infrastructure assets is earth retaining structures, among which is the reinforced soil structures, a technology that has beheld a significant increase in their number within the retaining walls inventory over the past four decades. Lateral displacement in reinforced soil walls is a major indicator of the performance of reinforced soil structures that has been extensively used by practitioners to judge the structural integrity of their walls in both the short and long terms. This indicator reflects the level of structural vulnerability, which can subsequently reflect the level of risk associated with structure failure, where failure is usually defined for reinforced soil walls as the condition when the applied loads are larger than the overall strength of individual structural components (Lazarte and Baecher 2003). This condition is referred to as the Ultimate Limit State (or Strength Limit State) in design codes (*e,g.*, AASHTO 2017).

Several efforts have been made to develop a reliable and simple method to estimate the lateral displacement of geosynthetic-reinforced soil walls. Table 1 compiles several analytical and empirical methods developed to estimate maximum lateral displacement and the variables used by each method. These methods are summarized in Scotland (2016), Scotland *et al.* (2016), Xiao *et al.* (2016), and Khosrojerdi *et al.* (2016). Bathurst *et al.* (2010) reviewed lateral displacement limits specified by 11 design guidelines for geosynthetic-reinforced soil structures. In their study, they compared the lateral displacements measured for a number of wall case studies to limits specified by the various guidelines. It was concluded that the method developed by Christopher *et al.* (1990), and adopted by FHWA (Berg *et al.* 2009) and AASHTO (2017), provided a reasonable upper limit in most cases for end-of-construction movements for walls constructed on firm foundations. However, both the vertical spacing of the reinforcement vertical spacing and the facing varied considerably in the walls evaluated. Bathurst *et al.* (2010) also evaluated a careful set of full-scale wall tests that revealed that end-of-construction lateral displacements are influenced by both compaction effort and global reinforcement stiffness when other influencing parameters remain unchanged. This effort is somewhat related to changing the spacing of reinforcements with the same modulus. In this case, the wall global stiffness would increase proportionally to the decreased spacing, as reviewed later in this section.

Table 1. Overview of existing lateral displacement prediction methods for geosynthetic-reinforced soil structures

No.	Reference	Variables
1	Allen and Bathurst (2015)	J, φ, c, q, S_v, γ, H
2	Bathurst (2002)	H, q, γ
3	Chew and Mitchell (1994)	J, S_v, L, H, α
4	Christopher et al. (1990)	Reinforcement type, L, H
5	Giroud (1989)	J, φ, q, S_v, γ, H, L
6	Lee (2000)	Face type, S_v, J, E_s
7	Jewell and Milligan (1989)	J, φ, q, S_v, γ, H, ψ
8	Wu (1994)	J, φ, q, S_v, γ, H, L
9	Wu and Pham (2010)	J, φ, q, S_v, γ, H, ψ, δ, β, γ_b, b'
10	Adams et al. (2011)	H, b_q, D_v

Notes:

J: Reinforcement tensile stiffness
φ: Reinforced fill angle of internal friction
c: Reinforced fill cohesion
q: Surcharge
S_v: Vertical reinforcement spacing
γ: Reinforced fill unit weight
H: Structure height as measured from the leveling pad
L: Reinforcement length
α: Backslope angle
E_s: Reinforced fill compression stiffness
ψ: Reinforced fill angle of dilation
δ: Angle of reinforcement-facing interface friction
β: Angle of soil-facing interface friction
γ_b: Equivalent unit of facing
b': Width of block facing
b_q: Width of vertical load on wall crest
D_v: Vertical displacement (*i.e.*, settlement) at wall crest

Khosrojerdi *et al.* (2016) evaluated six methods for prediction of maximum lateral displacements in geosynthetic-reinforced walls and abutments: (1) FHWA method developed by Christopher *et al.* (1990) and currently adopted by FHWA (Berg *et al.* 2009) and AASHTO (2017); (2) Geoservice Method developed by Giroud (1989); (3) CTI method developed by Wu (1994); (4) Jewell-Milligan Method developed by Jewell (1988) and Jewell and Milligan (1989); (5) Wu method (Wu and Pham 2010); and (6) Adams method (Adams *et al.* 2011). They compiled lateral displacement data measured in 17 geosynthetic-reinforced soil structures, which were used to assess the prediction accuracy of the six maximum lateral displacement prediction methods. Khosrojerdi *et al.* (2016) concluded that Adams method (Adams *et al.* 2011) is the most accurate among the six methods in predicting the maximum lateral displacement. Specifically, based on bias statistical analysis, Adams method was only found to be slightly unconservative, as it predicted lateral deformations that were on average 88% of the actual measured values. The method was also found to have good reliability when compared to the other six methods considered in the study with a low coefficient of variation (COV) value of 0.51 obtained for the 12 structures evaluated using that method. A reported limitation of this method is that the magnitude of the structure's vertical settlement must be known to predict the lateral deformations. Otherwise, estimates of vertical settlement would need to be made, which would potentially increase the uncertainty of this method. On the other hand, Khosrojerdi *et al.* (2016) concluded that FHWA method (Christopher *et al.* 1990) is highly conservative.

This paper presents a model for prediction of maximum lateral displacements in geosynthetic-reinforced soil walls. The proposed model is based on the lateral displacement prediction model originally developed by Christopher *et al.* (1990) and is used to date in FHWA (2009) and AASHTO (2017) to make rough estimates of the end-of-construction maximum lateral displacements. This Christopher *et al.* (1990) model was developed based on data generated from numerical simulations of reinforced soil structures.

2. DATABASE OF MONITORED STRUCTURES

Measuring lateral displacements during construction can be quite challenging, since the displacements take place gradually as construction progresses. To overcome the bias in lateral displacement evaluation, experimental geosynthetic-reinforced soil structures with reliable lateral displacement data were carefully selected to establish a database. Table 2 lists the structures for which lateral displacement data were compiled. Brief descriptions of these structures are presented as follows:

- Two walls constructed in Stockbridge, Georgia in 1994 (Ling and Leshchinsky 1996). These walls are the same structures. These walls were constructed with an *L/H* ratio of 0.3. While this L/H value is much smaller than that specified in AASHTO, it is still in the *L/H* range for which the Christopher *et al.* (1990) lateral deformation prediction model was developed. The lateral deformations of these walls were monitored during construction as well as after construction completion and application of fill surcharge. The vertical reinforcement spacing values in these walls were 0.4 and 0.8 m (1.3 and 2.6 ft). These structures were selected because of the availability to the authors of the displacement data collected during construction, which is deemed a rare dataset (Morsy *et al.* 2017; Morsy 2017).
- One wall reported by Bathurst *et al.* (1993), which was monitored after construction and, consequently, it provided data for calibration of surcharge-induced displacements only. This wall was constructed with an *L/H* ratio of 0.70 and vertical reinforcement spacing of 0.8 m. Additional displacement readings were recorded in this wall with time and constant surcharge after maximum surcharge was reached. Only displacement data due to increasing surcharge load was collected. This structure was selected to account for surcharge-induced lateral displacements (*i.e.*, post-construction lateral displacements).
- One wall reported by Salem *et al.* (2018), which was monitored at the end of construction and after applying surcharge loads. This wall was constructed with *L/H* ratio of 0.73 and vertical reinforcement spacing of 0.6 m. The lateral displacements were surveyed at various sections along the wall and the data were presented by maximum, minimum, and average measured envelopes. The variation in the surveying data was reported to have been due to looseness of some facing units. In addition to the surveying data, lateral displacements were estimated by integrating reinforcement strain data, which matched well with the minimum displacement envelope measured by surveying. Accordingly, the data corresponding to the minimum lateral displacement envelope were used in this study since they appear to be the most representative to the actual displacement experienced by the wall due to the internal deformation of the reinforced soil mass.
- Three walls reported by Hatami and Bathurst (2006), which were constructed with three different geogrid reinforcement types. The walls were constructed in an experimental facility using the same construction procedure. The three walls were constructed with *L/H* ratios of 0.62 and with vertical reinforcement spacings of 0.6 m.

Table 2. A summary of monitored structures used in the study

No.	*H* (m)	*L/H*	Facing Type	Backfill Type	Reinforcement Type	*J* (kN/m)	S_v (m)	Reference
1	6.80	0.30	Modular-Block	Sand	Geogrids	1025	0.40	Ling and Leshchinsky (1996); Morsy *et al.* (2017)
2	6.80	0.30	Modular-Block	Sand	Geogrids	1569	0.80	
3	6.14	0.70	Modular-Block	Sand	Geogrids	375	0.80	Bathurst *et al.* (1993)
4	4.40	0.73	Modular-Block	Sand	Geogrids	540	0.60	Salem *et al.* (2018)
5	3.60	0.62	Modular-Block	Sand	Geogrids	115	0.60	Hatami and Bathurst (2006)
6	3.60	0.62	Modular-Block	Sand	Geogrids	56.5	0.60	
7	3.60	0.62	Modular-Block	Sand	Geogrids	57	0.60	

3. MODEL DEVELOPMENT

As mentioned earlier, the model developed in this study takes the Christopher *et al.* (1990) maximum lateral displacement model adopted in AASHTO (2017) as initial basis. The lateral displacement model in the AASHTO (2017) can be written as follows:

$\delta_{max} = \frac{\delta_R H}{75}$ for walls with “extensible” reinforcements Eq. (1a)

$\delta_{max} = \frac{\delta_R H}{150}$ for walls with “inextensible” reinforcements Eq. (1b)

where δ_{max} is the maximum lateral deformation of reinforced soil wall, and *H* is the wall height measured from the top of the leveling pad on which the facing rests, and δ_R is a dimensionless reinforced soil wall deformation coefficient and is function of the reinforcement length to wall height ratio, *L/H*. The coefficient δ_R can be expressed as follows:

$$\delta_R = 11.81\left(\frac{L}{H}\right)^4 - 42.25\left(\frac{L}{H}\right)^3 + 57.16\left(\frac{L}{H}\right)^2 - 35.45\left(\frac{L}{H}\right) + 9.471 \quad \text{Eq. (2)}$$

where L is the reinforcement length. The relationship between the coefficient δ_R and *L/H* can be represented graphically as shown in Figure 1.

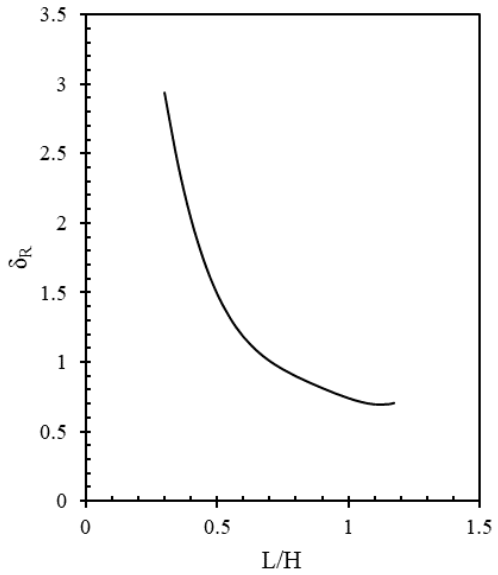

Figure 1. Variation of the reinforced soil wall deformation coefficient, δ_R, with *L/H* ratio (redrawn after AASHTO 2017)

The basis for having two forms of the equation (*i.e.*, for walls with "extensible" and "inextensible" reinforcements) pertains to the global stiffness of the wall, S_r, which is the average reinforcement tensile stiffness over the wall face area. The global stiffness can be expressed as follows:

$$S_r = \frac{1}{H}\sum_{i=1}^{n} J_i \qquad \text{Eq. (3)}$$

where J_i is the reinforcement tensile stiffness of the i^{th} reinforcement layer and n is the total number of layers in the wall. For walls with reinforcements of the same tensile stiffness, J, placed uniformly over the wall height at the same vertical spacing, S_v, the global stiffness can be written as follows:

$$S_r = \frac{J}{S_v} \qquad \text{Eq. (4)}$$

The Christopher *et al.* (1990) model uses *L/H* ratio (ranging between 0.3 and 1.175) and the reinforcement type. It should be noted that this equation was developed to predict the maximum lateral displacement of a wall during its construction, which is rarely measured in practice. While this model does not directly predict the additional lateral displacement that can take place upon the application of surcharge loads, Christopher *et al.* (1990) stated that for a 6-m (20-ft) high wall, each additional 20 kPa (417 psf) of surcharge load results in a 25% increase in the relative deformation.

The proposed model modified Christopher *et al.* (1990) model by introducing the effect of global stiffness, S_r, of the structure, which was the genesis of the original model development, and the effect of surcharge load. The proposed modifications include introduction of S_r to the prediction model and introduction of a surcharge-induced component. The resulting formulation is as follows:

$$\delta_{max} = \left(\frac{F_b \delta_R H}{F_f \frac{S_r}{p_o}}\right)\left(1 + 1.25\frac{q}{p_o}\right) \qquad \text{for walls with "extensible" reinforcements} \qquad \text{Eq. (5)}$$

where δ_R is the dimensionless reinforced soil wall deformation coefficient as defined in the original model (Eq. 2); q is the magnitude of surcharge; p_o is atmospheric pressure introduced in the equation to normalize S_r and q; F_f and F_b are dimensionless factors to account for face type and face batter, respectively. The second term (multiplier) in the developed model includes in turn two sub-terms: the unity sub-term that corresponds to the maximum lateral displacement at the end of construction, and the surcharge sub-term that corresponds to the maximum lateral displacement induced by surcharge only. Note that the surcharge sub-term was developed based on Christopher *et al.* (1990) recommendation that every 20 kPa (0.2 p_o) of surcharge load results in a 25% increase in the lateral displacement, as mentioned earlier.

Lateral facing displacements are usually estimated by integrating reinforcement strains, which include two components: (1) reinforcement strains within the soil driving wedge; and (2) reinforcement strains within the restraining soil zone (Jewell

and Milligan 1989). The former component represents the major contributor to the integrated reinforcement strains and lateral facing displacements. Estimating reinforcement strains can be quite complex since the location and shape of the internal failure surface may be different than the idealized surfaces usually assumed in design, such as Rankine's failure surface in geosynthetic-reinforced soil walls (AASHTO 2017). In fact, the location and shape of failure surfaces depend on several wall properties, as has been observed in numerous instrumented wall cases. However, due to the complexity of predicting the geometry of the failure surfaces, idealized failure surfaces may be used. The idealized design surfaces have been used in practice to date and are deemed by practitioners to be conservative since they are usually deeper than the locus of maximum reinforcement tensile stresses identified in field. Additionally, a deeper potential failure plane increases the width of the driving soil wedge, which increases the reinforcement strained length used in estimating lateral facing displacements. Also, the shape and location of the potential failure surface also changes with the face batter. Specifically, the width of the driving soil wedge decreases with increasing the face batter, which results in smaller tensile stresses in reinforcements and smaller strained reinforcement lengths. Since Christopher *et al.* (1990) model was developed for walls with zero face batter, a reduction factor, F_b, was introduced in the proposed model herein to account for face batter in reinforced soil walls. This reduction factor was introduced to the model to facilitate calibration against field data so that the model is not affected by seemingly lower lateral displacements measured in walls with considerable face batter. However, it is conservative to consider this reduction factor as 1.0 in design.

Leshchinsky and Boedeker (1989) developed design charts that facilitate identifying the geometry of the potential failure surface in reinforced soil structures considering face batter using limit equilibrium. The reduction factor was developed to account for the strained reinforcement length (the driving soil wedge width) in reinforced soil walls with face batter. The reduction factor represents the ratio of average strained reinforcement length of a wall with face batter 1H:mV to the average strained reinforcement length in a wall with vertical face ($m \rightarrow \infty$). Figure 2 shows the reduction factor F_b versus face batter for walls with soil friction angles of 20, 30, and 40 degrees. As shown in the figure, the reduction factor various slightly from 0.947 to 1.00 for walls with face batter as large as 1H:10V (equivalent to batter angle of approximately 6 degrees).

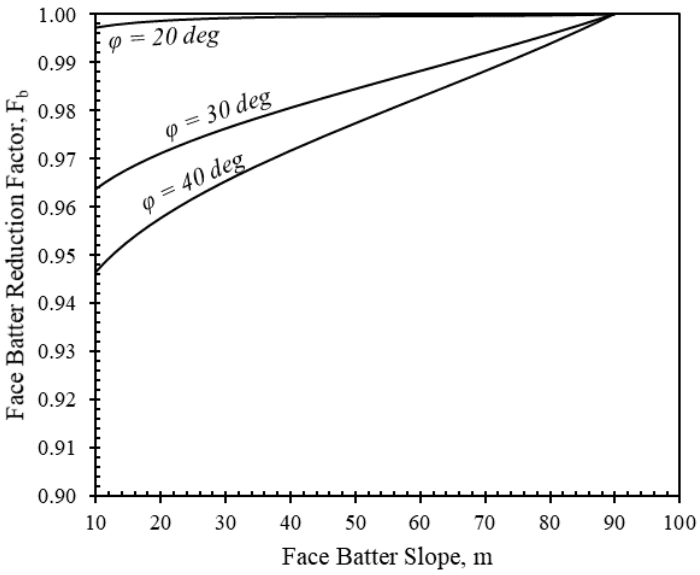

Figure 2. Face batter reduction factor, F_b

Lateral displacements in reinforced soil structures can be divided into three different deformations: (1) face deformation; (2) internal deformation; and (3) global deformation (Scotland 2016; Scotland *et al.* 2016). The internal deformation occurs to facing elements regardless the reinforcement strain. This deformation is usually encountered the most in wrapped-around reinforcement facings where facings sag outward increasing the total lateral displacements. Internal deformation occurs to reinforcement elements as they strain axially. This deformation has the largest contribution to the total lateral displacements. Global deformation occurs to the entire reinforced soil structure due to sliding and/or overturning. The contribution of this deformation to the total lateral displacement is governed by the factors controlling the external stability of the structure, among which is the *L/H* ratio. Consequently, the lateral displacement model proposed in this paper introduced a factor, F_f, that accounts for the effect of facing type on the lateral displacements in reinforced soil walls. Since this paper is focused on the lateral displacements in geosynthetic-reinforced soil structures with segmental block facings only, the value of this factor was defined only for this type of structures, where F_f = 80. Zornberg *et al.* (2018, 2019)

proposed $F_f = 50$, which was developed as a lower bound that could be used with walls with wrapped-around reinforcement facings (*i.e.*, with the most flexible facing types).

4. MODEL EVALUATION

Figure 3 presents the predicted versus measured maximum displacements for the four structures evaluated in this study. For those walls whose displacements were only measured post construction (including surcharge-induced displacements), Eq. (5) was used but without the unity term (*i.e.*, only change in maximum lateral displacements measured after construction completion and due to surcharge is computed). Since reinforcements creep with time due to reduction in their tensile stiffnesses, J, the magnitudes of lateral displacements increase with time under constant load. The developed model can predict long-term lateral displacements by using global stiffness, S_r, values that correspond to creep reinforcement stiffness values.

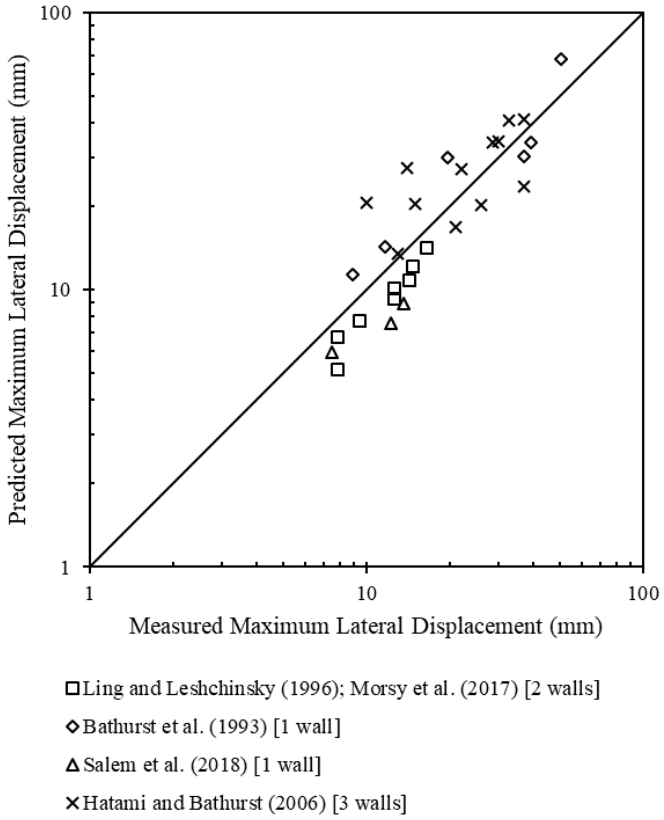

Figure 3. Predicted versus measured maximum displacements using the proposed model

The comparison shown in Figure 3 reveals good agreement between the lateral displacements predicted using the proposed modified method and field displacement measurements. Consequently, the modifications proposed for the equations are deemed adequate for use in practice to predict lateral displacements in geosynthetic-reinforced soil structures with segmental-block facings.

5. CONCLUSION

This paper presents an empirical model developed to predict maximum lateral displacements in geosynthetic-reinforced soils walls with segmental-block facings. The model used as a basis the current model in AASHTO (2017), which I used to provide rough estimates to the maximum lateral displacements during construction. The proposed model incorporates the global stiffness of the structure and provides estimates to the lateral displacements of walls subject to surcharge loads. Lateral displacement monitoring data were compiled from carefully selected reinforced soil walls to develop the model. Finally, predicted lateral displacement data were plotted against corresponding measured data. It was observed that the proposed model is suitable for geosynthetic-reinforced soil walls with generic surcharge loads. The proposed model should

only be adopted for the case of walls constructed using high quality backfill and employing high quality design and construction protocols.

6. ACKNOWLEDGEMENTS

This research was partly supported by the National Cooperative Highway Research Program (NCHRP) under project NCHRP 24-41. The opinions presented in this paper are exclusively those of the authors and not necessarily those of the NCHRP.

7. REFERENCES

AASHTO. (2017). AASHTO LRFD bridge design specifications, 8th Ed., Washington, DC.

Adams, M., Nicks, J., Stabile, T.,Wu, J. T., Schlatter, W., and Hartmann, J. (2011). "Geosynthetic reinforced soil integrated bridge system interim implementation guide." Rep. No. FHWA-HRT-11-026, Federal Highway Administration, Washington, DC.

Allen, T. M., and Bathurst, R. J. (2015). Improved simplified method for prediction of loads in reinforced soil walls. Journal of Geotechnical and Geoenvironmental Engineering, 141, No. 11, 04015049.

Bathurst, R. J., Allen, T. M., and Walters, D. L. (2002). Short-term strain and deformation behaviour of geosynthetic walls at working stress conditions. Geosynthetics International, 9, No. 5–6, 451–482.

Bathurst, R. J., Jarrett, P. M., and Benjamin, D. J. (1993). "A database of results from an incrementally constructed geogrid-reinforced soil wall test." Proc., Soil Reinforcement: Full Scale Experiments of the 80s, ISSMFE/ENPC, Paris, 401–430.

Bathurst, R.J., Miyata, Y. and Allen, T.M. 2010. Invited keynote paper, Facing displacements in geosynthetic reinforced soil walls. Earth Retention Conference 3 (ER2010)., ASCE Geo-Institute, Bellevue, Washington 1-4 August, 18p.

Berg, R. R., Christopher, B. R., Samtani, N. C., and Berg, R. R. (2009). Design of mechanically stabilized earth walls and reinforced soil slopes–Volume I (No. FHWA-NHI-10-024). United States. Federal Highway Administration.

Chew, S. H., and Mitchell, J. K. (1994). Deformation evaluation procedure for reinforced soil walls. Proceedings of 5th International Conference on Geotextiles, Geomembranes and Related Products, Singapore, September 1994, pp. 171–176.

Christopher, B. R., Gill, S. A., Giroud, J. P., Mitchell, J. K., Schlosser, F., and Dunnicliff, J. (1990). "Reinforced soil structures. Vol. 1: Design and construction guidelines." Rep. No. FHWA-RD 89-043, Federal Highway Administration, Washington, DC.

Giroud, J. P. (1989). "Geotextile engineering workshop-design examples." Rep. No. FHWA-HI-89-002, Federal Highway Administration, Washington, DC.

Hatami, K., and Bathurst, R. J. (2005). "Development and verification of a numerical model for the analysis of geosynthetic-reinforced soil segmental walls under working stress conditions." Can. Geotech. J., 42(4), 1066–1085.

Jewell, R. A. (1988). "Reinforced soil wall analysis and behavior." The application of polymeric reinforcement in soil retaining structures, Kluwer, Netherlands.

Jewell, R. A., and Milligan, G. W. E. (1989). "Deformation calculation for reinforced soil walls." Proc., 12th Int. Conf. on Soil Mechanics and Foundation Engineering, Vol. 2, Taylor & Francis, Abingdon, U.K., 1259–1262.

Khosrojerdi, M., Xiao, M., Qiu, T., and Nicks, J. (2016). Evaluation of prediction methods for lateral deformation of GRS walls and abutments. Journal of Geotechnical and Geoenvironmental Engineering, 143(2), 06016022.

Lazerte C., and Baecher, G.B. (2003). "LRFD for Soil Nailing Design and Specifications." LSD2003: International Workshop on Limit State Design in Geotechnical Engineering Practice, Cambridge, Massachusetts, 26 June 2003.

Lee, W. F. (2000). Internal Stability Analyses of Geosynthetic Reinforced Retaining Walls, PhD thesis, University of Washington, Seattle, Washington, USA.

Leshchinsky, D., and Boedeker, R. H. (1989). Geosynthetic reinforced soil structures. Journal of Geotechnical Engineering, 115(10), 1459-1478.

Ling, P., and Leshchinsky, D. (1996). MESA Walls: Field Data Reduction, finite element analysis, and prelimnary design recommendations, Tensar Earth Technologies, Inc, Atlanta, GA (unpublished report)

Morsy, A.M. (2017), Evaluation of Soil-Reinforcement Composite Interaction in Geosynthetic-Reinforced Soil Structures, Ph.D. Dissertation, Department of Civil, Architectural, and Environmental Engineering, The University of Texas at Austin, Austin, Texas, The United States of America, 635p.

Morsy, A. M., Leshchinsky, D., and Zornberg, J. G. (2017). Effect of Reinforcement Spacing on the Behavior of Geosynthetic-Reinforced Soil. In Geotechnical Frontiers 2017 (pp. 112-125).

Salem, M. A., Hammad, M. A., and Amer, M. I. (2018). Field monitoring and numerical modeling of 4.4 m-high mechanically stabilized earth wall. Geosynthetics International, 25(5), 545-559.

Scotland, I. (2016). Analysis of horizontal deformations to allow the optimisation of geogrid reinforced structures (Doctoral dissertation, © Ian Scotland).

Scotland, I., Dixon, N., Frost, M. W., Fowmes, G. J., and Horgan, G. (2016). Modelling deformation during the construction of wrapped geogrid reinforced structures. Geosynthetics International, 2016, 23, No. 3

Wu, J. T. (1994). “Design and construction of low cost retaining walls: The next generation in technology.” Rep. No. CTI-UCD-1-94, Colorado Transportation Institute, Denver, CO.

Wu, J., and Pham, T. (2010). An analytical model for calculating lateral movement of a geosynthetic-reinforced soil (GRS) wall with modular block facing. International Journal of Geotechnical Engineering, 4(4), 527-535.

Xiao, M., Qui, T., Khosrojerdi, M., Basu, P., and Withiam, J. L. (2016). Synthesis and evaluation of the service limit state of engineered fills for bridge support (No. FHWA-HRT-15-080). United States. Federal Highway Administration. Office of Infrastructure Research and Development.

Zornberg, J.G., Morsy, A.M., Kouchaki, B.M., Christopher, B.R., Leshchinsky, D., Han, J., Tanyu, B.F., Gebremariam, F.T., Shen, P., and Jiang, Y. (2019), Proposed Refinements to Design Procedures for Geosynthetic Reinforced Soil (GRS) Structures in AASHTO LRFD Bridge Design Specifications. NCHRP Web-Only Document 260, National Cooperative Highway Research Program (NCHRP), Transportation Research Board of the National Academies, 69p. https://doi.org/10.17226/25416

Zornberg, J.G., Morsy, A.M., Kouchaki, B.M., Christopher, B.R., Leshchinsky, D., Han, J., Tanyu, B.F., Gebremariam, F.T., Shen, P., and Jiang, Y. (2018), Defining the Boundary Conditions for Composite Behavior of Geosynthetic Reinforced Soil (GRS) Structures. Project NCHRP 24-41, National Cooperative Highway Research Program (NCHRP), Transportation Research Board of the National Academies, 1006p.